ESHELBY INCLUSION OF ARBITRARY SHAPE IN ISOTROPIC ELASTIC
MATERIALS WITH A PARABOLIC BOUNDARY

Xu Wang, Liang Chen and Peter Schiavone

msp

ESHELBY INCLUSION OF ARBITRARY SHAPE IN ISOTROPIC ELASTIC MATERIALS WITH A PARABOLIC BOUNDARY

Xu Wang, Liang Chen and Peter Schiavone

We employ analytic continuation and conformal mapping techniques to derive analytic solutions for Eshelby's problem of an elastic inclusion of arbitrary shape in an isotropic elastic plane with parabolic boundary. The region of the physical (z-) plane lying below the parabola is mapped (conformally) onto the lower half of the image (ξ-) plane. The corresponding boundary value problem is then analyzed in the ξ-plane. A second conformal mapping, which maps the exterior of the region occupied by the (simply-connected) inclusion in the ξ-plane onto the exterior of the unit circle, is then used to construct an auxiliary function of ξ which, when used together with analytic continuation, allows us to extend our analysis to an inclusion of arbitrary shape.

1. Introduction

Eshelby's classic problem concerning a subdomain (inclusion) undergoing uniform stress-free eigen-strains continues to inspire researchers working in several areas of materials science (see, for example, [Zhou et al. 2013] for a recent review). The two-dimensional Eshelby's problem of an inclusion of arbitrary shape located in the vicinity of a straight boundary has been well-studied and is now considered to be solved [Ru 1999; Ru 2000; Ru 2003; Wang 2004; Wang and Schiavone 2015; Wang and Zhou 2014]. In contrast, there are relatively few studies pertaining to the corresponding problem of an Eshelby inclusion of arbitrary shape lying near an open *curvilinear* boundary. The importance of this class of problem can be illustrated, for example, by considering the case when the inclusion lies in an elastic plane with parabolic boundary. In this case, the parabola represents the blunt crack tip of a crack present in some fractured material and the inclusion perhaps a transformation strain spot of arbitrary shape. In this way, the corresponding model can be used to study the shielding or anti-shielding effect of the transformation strain spot on a nearby crack.

In this paper, we do, in fact, consider the Eshelby's problem of an inclusion of arbitrary shape in an isotropic elastic plane with parabolic boundary. Our approach differs from that used by [Ru 1999] for the analogous problem involving a straight boundary (as mentioned above) in that instead of analyzing the corresponding boundary value problem in the physical plane, our analysis is confined to the image plane. Specifically, the region below the parabola is first mapped onto the lower half-plane in the image (ξ-) plane in which the boundary value problem is then analyzed. A conformal mapping function which maps the exterior of the region occupied by the (simply-connected) inclusion in the ξ-plane onto the exterior of the unit circle [Savin 1961; England 1971] is then used to construct an auxiliary function $D(\xi)$ with which the problem can be solved using analytic continuation.

The paper is structured as follows. Muskhelishvili's complex variable formulations for two-dimensional isotropic elasticity are given in Section 2. Analytic solutions to the corresponding problems involving in-plane and anti-plane shear eigenstrains are derived in Section 3. Several specific examples are presented in Section 4 to illustrate the method. Finally, conclusions are drawn in Section 5.

2. Complex variable formulations

For plane deformations of an isotropic elastic material, the stresses $(\sigma_{11}, \sigma_{22}, \sigma_{12})$, displacements (u_1, u_2) and stress functions (ϕ_1, ϕ_2) can be expressed in terms of two analytic functions $\varphi(z)$ and $\psi(z)$ of the complex variable $z = x_1 + \mathrm{i}x_2$ as follows [Muskhelishvili 1953; Ting 1996]:

$$\sigma_{11} + \sigma_{22} = 2\left(\varphi'(z) + \overline{\varphi'(z)}\right), \quad \sigma_{22} - \sigma_{11} + 2\mathrm{i}\sigma_{12} = 2\left(\bar{z}\varphi''(z) + \psi'(z)\right), \tag{1}$$

$$2\mu(u_1 + \mathrm{i}u_2) = \kappa\varphi(z) - z\overline{\varphi'(z)} - \overline{\psi(z)}, \quad \phi_1 + \mathrm{i}\phi_2 = \mathrm{i}\left(\varphi(z) + z\overline{\varphi'(z)} + \overline{\psi(z)}\right), \tag{2}$$

where $\kappa = 3 - 4\nu$ for plane strain, $\kappa = (3-\nu)/(1+\nu)$ for plane stress and $\mu, \nu (0 \le \nu \le 1/2)$ are the shear modulus and Poisson's ratio, respectively. In addition, the stresses are related to the stress functions through

$$\begin{aligned} \sigma_{11} &= -\phi_{1,2}, & \sigma_{12} &= \phi_{1,1}, \\ \sigma_{21} &= -\phi_{2,2}, & \sigma_{22} &= \phi_{2,1}. \end{aligned} \tag{3}$$

Under the assumption of anti-plane shear deformations of an isotropic elastic material, the two shear stress components $(\sigma_{31}, \sigma_{32})$, the out-of-plane displacement u_3 and the stress function ϕ_3 can be expressed in terms of a single analytic function $f(z)$ of the complex variable $z = x_1 + \mathrm{i}x_2$ as

$$\sigma_{32} + \mathrm{i}\sigma_{31} = \mu f'(z), \quad \phi_3 + \mathrm{i}\mu u_3 = \mu f(z), \tag{4}$$

where the two stress components can be expressed in terms of the stress function ϕ_3 as

$$\sigma_{32} = \phi_{3,1}, \quad \sigma_{31} = -\phi_{3,2}. \tag{5}$$

3. An inclusion in a region with parabolic boundary

As shown in Figure 1, we consider an isotropic elastic material that occupies the region:

$$x_2 \le ax_1^2, \quad a \ge 0, \tag{6}$$

the traction-free boundary of which is a parabola described by

$$x_2 = ax_1^2. \tag{7}$$

The parabola reduces to a semi-infinite crack when $a \to \infty$ and a straight boundary when $a = 0$. The isotropic plane with parabolic boundary contains an internal subdomain undergoing uniform in-plane and anti-plane stress-free eigenstrains $(\varepsilon_{11}^*, \varepsilon_{22}^*, \varepsilon_{12}^*)$ and $(\varepsilon_{31}^*, \varepsilon_{32}^*)$. Let S_2 and S_1 denote, respectively, the subdomain (the Eshelby inclusion) and its exterior while Γ denotes the perfectly bonded interface separating S_2 and S_1. In what follows, the subscripts 1 and 2 refer to S_1 and S_2, respectively.
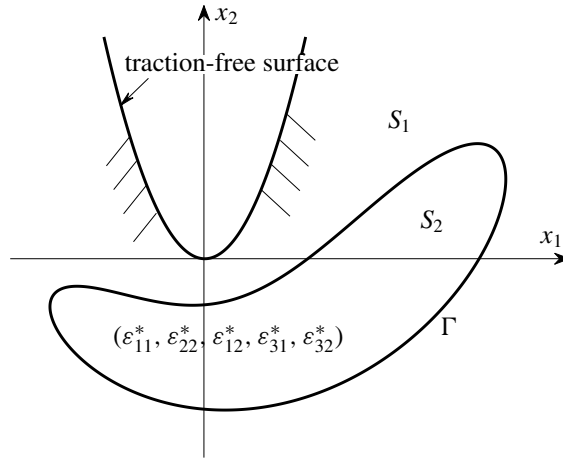
**Figure 1.** An Eshelby inclusion of arbitrary shape in an isotropic elastic plane with a parabolic boundary.

We introduce the following conformal mapping function [Ting et al. 2001]:

$$z = \omega(\xi) = \xi + \mathrm{i}a\xi^2, \quad \xi = \omega^{-1}(z) = \frac{\sqrt{1 + 4\mathrm{i}az} - 1}{2\mathrm{i}a}, \quad \mathrm{Im}\,\xi \le 0. \tag{8}$$

With reference to Figure 2, the parabola itself is mapped onto the real axis in the ξ-plane and the region below the parabola onto the lower half ξ-plane. The inclusion $z \in S_2$ is mapped onto $\xi \in \Omega_2$, the matrix $z \in S_1$ onto $\xi \in \Omega_1$ and the interface $z \in \Gamma$ is mapped onto $\xi \in L$. The elliptical shape of L in Figure 2 is chosen simply for illustrative purposes; in fact L may be of arbitrary shape. For convenience and without loss of generality, we write

$$\varphi_j(\xi) = \varphi_j(\omega(\xi)), \quad \psi_j(\xi) = \psi_j(\omega(\xi)), \quad f_j(\xi) = f_j(\omega(\xi)), \quad j = 1, 2.$$

In what follows, we derive analytic solutions in the case of both in-plane and anti-plane eigenstrains.
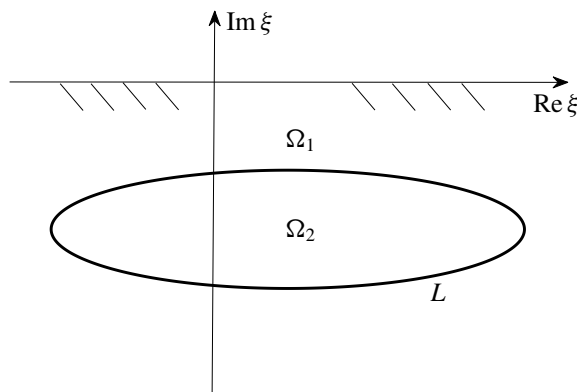
Figure 2. The problem in the ξ-plane.

3.1. *In-plane eigenstrains* $(\varepsilon_{11}^*, \varepsilon_{22}^*, \varepsilon_{12}^*)$. In this case, the boundary value problem in the ξ-plane takes the following form:

$$\kappa\varphi_1(\xi) - \frac{\omega(\xi)}{\overline{\omega'(\xi)}}\,\overline{\varphi_1'(\xi)} - \overline{\psi_1(\xi)} = \kappa\varphi_2(\xi) - \frac{\omega(\xi)}{\overline{\omega'(\xi)}}\,\overline{\varphi_2'(\xi)} - \overline{\psi_2(\xi)} + 2\mu[\delta_1\omega(\xi) + (\delta_2 + \mathrm{i}\delta_3)\overline{\omega(\xi)}],$$
(9a)
$$\varphi_1(\xi) + \frac{\omega(\xi)}{\overline{\omega'(\xi)}}\,\overline{\varphi_1'(\xi)} + \overline{\psi_1(\xi)} = \varphi_2(\xi) + \frac{\omega(\xi)}{\overline{\omega'(\xi)}}\,\overline{\varphi_2'(\xi)} + \overline{\psi_2(\xi)}, \quad \xi \in L;$$

$$\varphi_1(\xi) + \frac{\omega(\xi)}{\overline{\omega'(\xi)}}\,\overline{\varphi_1'(\xi)} + \overline{\psi_1(\xi)} = 0, \quad \mathrm{Im}\,\xi = 0^-;$$
(9b)

$$\varphi_1(\xi) \cong O(1), \quad \psi_1(\xi) \cong O(1), \quad |\xi| \to \infty,$$
(9c)

where the real numbers δ_1, δ_2 and δ_3 are related to the in-plane eigenstrains through

$$\delta_1 = \frac{\varepsilon_{11}^* + \varepsilon_{22}^*}{2}, \quad \delta_2 = \frac{\varepsilon_{11}^* - \varepsilon_{22}^*}{2}, \quad \delta_3 = \varepsilon_{12}^*.$$
(10)

After straightforward algebraic manipulations, the two interface conditions in (9a) can be expressed equivalently as

$$\varphi_1(\xi) = \varphi_2(\xi) + \frac{2\mu}{\kappa + 1}[\delta_1\omega(\xi) + (\delta_2 + \mathrm{i}\delta_3)\overline{\omega(\xi)}],$$
(11)
$$\psi_1(\xi) + \frac{\overline{\omega(\xi)}}{\omega'(\xi)}[\varphi_1'(\xi) - \varphi_2'(\xi)] = \psi_2(\xi) - \frac{2\mu}{\kappa + 1}[\delta_1\overline{\omega(\xi)} + (\delta_2 - \mathrm{i}\delta_3)\omega(\xi)], \quad \xi \in L.$$

If $z \in S_2$ is simply connected, $\xi \in \Omega_2$ is also simply connected. Thus, there exists a conformal mapping $\xi = w(\eta)$ that maps the exterior of Ω_2 in the ξ-plane onto the exterior of the unit circle in the η-plane [Savin 1961; England 1971]. As a result, an auxiliary function $D(\xi)$ can be constructed as follows:

$$\overline{\omega(\xi)} = \bar{\xi} - \mathrm{i}a\bar{\xi}^2 = \bar{w}\Big(\frac{1}{w^{-1}(\xi)}\Big) - \mathrm{i}a\Big[\bar{w}\Big(\frac{1}{w^{-1}(\xi)}\Big)\Big]^2 = D(\xi), \quad \xi \in L.$$
(12)

In addition, the auxiliary function $D(\xi)$ is analytic in the exterior of Ω_2 except at the point at infinity, where it has a pole of finite degree, namely

$$D(\xi) = P(\xi) + O(\xi^{-1}), \quad |\xi| \to \infty,$$
(13)

where $P(\xi)$ is a polynomial of order $2N$ in ξ if $\xi = w(\eta)$ is a polynomial of order N in $1/\eta$.

Using (12), Equation (11) can be rewritten as

$$\varphi_1(\xi) - \frac{2\mu}{\kappa + 1}\big(\delta_1\omega(\xi) + (\delta_2 + \mathrm{i}\delta_3)D(\xi)\big) = \varphi_2(\xi),$$
(14)
$$\psi_1(\xi) + \frac{2\mu}{\kappa + 1}\Big[2\delta_1 D(\xi) + (\delta_2 + \mathrm{i}\delta_3)\frac{D(\xi)D'(\xi)}{\omega'(\xi)} + (\delta_2 - \mathrm{i}\delta_3)\omega(\xi)\Big] = \psi_2(\xi), \quad \xi \in L.$$

The asymptotic behavior of $D(\xi)D'(\xi)/\omega'(\xi)$ at infinity is given by

$$\frac{D(\xi)D'(\xi)}{\omega'(\xi)} = Q(\xi) + O(\xi^{-1}), \quad |\xi| \to \infty,$$
(15)

where $Q(\xi)$ is a polynomial of order $2N(2N-1)$ in ξ if $\xi = w(\eta)$ is a polynomial of order N in $1/\eta$. In view of (13) and (15), Equation (14) can be recast into the form

$$\varphi_1(\xi) - \frac{2\mu}{\kappa+1}(\delta_2 + i\delta_3)\big(D(\xi) - P(\xi)\big) = \varphi_2(\xi) + \frac{2\mu}{\kappa+1}\big(\delta_1\omega(\xi) + (\delta_2 + i\delta_3)P(\xi)\big),$$

$$\psi_1(\xi) + \frac{2\mu}{\kappa+1}\bigg[2\delta_1\big(D(\xi) - P(\xi)\big) + (\delta_2 + i\delta_3)\bigg(\frac{D(\xi)D'(\xi)}{\omega'(\xi)} - Q(\xi)\bigg)\bigg]$$

$$= \psi_2(\xi) - \frac{2\mu}{\kappa+1}\big((\delta_2 - i\delta_3)\omega(\xi) + 2\delta_1 P(\xi) + (\delta_2 + i\delta_3)Q(\xi)\big), \quad \xi \in L. \quad (16)$$

We now define two auxiliary functions $\Phi(\xi)$ and $\Psi(\xi)$ by

$$\Phi(\xi) = \begin{cases} \varphi_1(\xi) - \dfrac{2\mu}{\kappa+1}(\delta_2 + i\delta_3)\big(D(\xi) - P(\xi)\big), & \xi \in \Omega_1, \\[2ex] \varphi_2(\xi) + \dfrac{2\mu}{\kappa+1}\big(\delta_1\omega(\xi) + (\delta_2 + i\delta_3)P(\xi)\big), & \xi \in \Omega_2, \end{cases}$$

$$\Psi(\xi) = \begin{cases} \psi_1(\xi) + \dfrac{2\mu}{\kappa+1}\bigg[2\delta_1\big(D(\xi) - P(\xi)\big) + (\delta_2 + i\delta_3)\bigg(\dfrac{D(\xi)D'(\xi)}{\omega'(\xi)} - Q(\xi)\bigg)\bigg], & \xi \in \Omega_1, \\[2ex] \psi_2(\xi) - \dfrac{2\mu}{\kappa+1}\big((\delta_2 - i\delta_3)\omega(\xi) + 2\delta_1 P(\xi) + (\delta_2 + i\delta_3)Q(\xi)\big), & \xi \in \Omega_2. \end{cases} \quad (17)$$

It is seen from the above definition and (16) that $\Phi(\xi)$ and $\Psi(\xi)$ are continuous across L and then analytic in the lower half ξ-plane including the point at infinity. Now the traction-free condition in (9b) can be given in terms of $\Phi(\xi)$ and $\Psi(\xi)$ as follows:

$$\Phi^-(\xi) + \frac{2\mu}{\kappa+1}(\delta_2 - i\delta_3)\frac{\omega(\xi)}{\bar{\omega}'(\xi)}\big(\overline{D}'(\xi) - \overline{P}'(\xi)\big) - \frac{2\mu}{\kappa+1}\bigg[2\delta_1\big(\overline{D}(\xi) - \overline{P}(\xi)\big) + (\delta_2 - i\delta_3)\bigg(\frac{\overline{D}(\xi)\overline{D}'(\xi)}{\bar{\omega}'(\xi)} - \overline{Q}(\xi)\bigg)\bigg]$$

$$+ \frac{3\mu}{\kappa+1}\frac{(\delta_3 + i\delta_2)\big(\overline{D'[i(2a)^{-1}]} - \overline{P'[i(2a)^{-1}]}\big)}{2a(1 - 2ia\xi)} + \frac{2\mu}{\kappa+1}\frac{(\delta_2 - i\delta_3)\overline{D[i(2a)^{-1}]D'[i(2a)^{-1}]}}{1 - 2ia\xi}$$

$$= -\overline{\Psi}^+(\xi) - \frac{\omega(\xi)}{\bar{\omega}'(\xi)}\overline{\Phi}'^+(\xi) - \frac{2\mu}{\kappa+1}(\delta_2 + i\delta_3)\big(D(\xi) - P(\xi)\big)$$

$$+ \frac{3\mu}{\kappa+1}\frac{(\delta_3 + i\delta_2)\big[\overline{D'[i(2a)^{-1}]} - \overline{P'[i(2a)^{-1}]}\big]}{2a(1 - 2ia\xi)} + \frac{2\mu}{\kappa+1}\frac{(\delta_2 - i\delta_3)\overline{D[i(2a)^{-1}]D'[i(2a)^{-1}]}}{1 - 2ia\xi},$$

$$\text{Im}\,\xi = 0. \quad (18)$$

The left and right sides of (18) are analytic in the lower and upper half-planes, respectively, including the point at infinity. By applying Liouville's theorem, we conclude that the left and right sides of (18) are identically zero. We thus arrive at the following expressions for $\Phi(\xi)$ and $\Psi(\xi)$:

$$\Phi(\xi) = -\frac{2\mu}{\kappa+1}(\delta_2 - \mathrm{i}\delta_3)\frac{\omega(\xi)}{\bar{\omega}'(\xi)}\big(\overline{D}'(\xi) - \overline{P}'(\xi)\big) + \frac{2\mu}{\kappa+1}\left[2\delta_1\big(\overline{D}(\xi) - \overline{P}(\xi)\big) + (\delta_2 - \mathrm{i}\delta_3)\left(\frac{\overline{D}(\xi)\overline{D}'(\xi)}{\bar{\omega}'(\xi)} - \overline{Q}(\xi)\right)\right]$$

$$- \frac{3\mu}{\kappa+1}\frac{(\delta_3 + \mathrm{i}\delta_2)\big(\overline{D'[\mathrm{i}(2a)^{-1}]} - \overline{P'[\mathrm{i}(2a)^{-1}]}\big)}{2a(1 - 2\mathrm{i}a\xi)} - \frac{2\mu}{\kappa+1}\frac{(\delta_2 - \mathrm{i}\delta_3)\overline{D[\mathrm{i}(2a)^{-1}]D'[\mathrm{i}(2a)^{-1}]}}{1 - 2\mathrm{i}a\xi},$$

$$\Psi(\xi) + \frac{\bar{\omega}(\xi)}{\omega'(\xi)}\Phi'(\xi) = -\frac{2\mu}{\kappa+1}(\delta_2 - \mathrm{i}\delta_3)\big(\overline{D}(\xi) - \overline{P}(\xi)\big)$$

$$+ \frac{3\mu}{\kappa+1}\frac{(\delta_3 - \mathrm{i}\delta_2)\big(D'[\mathrm{i}(2a)^{-1}] - P'[\mathrm{i}(2a)^{-1}]\big)}{2a(1 + 2\mathrm{i}a\xi)} + \frac{2\mu}{\kappa+1}\frac{(\delta_2 + \mathrm{i}\delta_3)D[\mathrm{i}(2a)^{-1}]D'[\mathrm{i}(2a)^{-1}]}{1 + 2\mathrm{i}a\xi},$$

$$\mathrm{Im}\,\xi \le 0. \quad (19)$$

It is not difficult to verify that $\Phi(\xi)$ is regular at $\xi = -\mathrm{i}/2a$. It follows from (17) and (19) that

$$\frac{\kappa+1}{2\mu}\varphi_1(\xi) = (\delta_2 + \mathrm{i}\delta_3)\big(D(\xi) - P(\xi)\big) - (\delta_2 - \mathrm{i}\delta_3)\frac{\omega(\xi)}{\bar{\omega}'(\xi)}\big(\overline{D}'(\xi) - \overline{P}'(\xi)\big)$$

$$+ 2\delta_1\big(\overline{D}(\xi) - \overline{P}(\xi)\big) + (\delta_2 - \mathrm{i}\delta_3)\left(\frac{\overline{D}(\xi)\overline{D}'(\xi)}{\bar{\omega}'(\xi)} - \overline{Q}(\xi)\right)$$

$$- \frac{3(\delta_3 + \mathrm{i}\delta_2)\big(\overline{D'[\mathrm{i}(2a)^{-1}]} - \overline{P'[\mathrm{i}(2a)^{-1}]}\big)}{4a(1 - 2\mathrm{i}a\xi)} - \frac{(\delta_2 - \mathrm{i}\delta_3)\overline{D[\mathrm{i}(2a)^{-1}]D'[\mathrm{i}(2a)^{-1}]}}{1 - 2\mathrm{i}a\xi},$$

$$\frac{\kappa+1}{2\mu}\psi_1(\xi) = -\frac{\kappa+1}{2\mu}\frac{\bar{\omega}(\xi)\varphi_1'(\xi)}{\omega'(\xi)} - 2\delta_1\big(D(\xi) - P(\xi)\big) - (\delta_2 + \mathrm{i}\delta_3)\left(\frac{D(\xi)D'(\xi)}{\omega'(\xi)} - Q(\xi)\right)$$

$$+ (\delta_2 + \mathrm{i}\delta_3)\frac{\bar{\omega}(\xi)}{\omega'(\xi)}\big(D'(\xi) - P'(\xi)\big) - (\delta_2 - \mathrm{i}\delta_3)\big(\overline{D}(\xi) - \overline{P}(\xi)\big)$$

$$+ \frac{3(\delta_3 - \mathrm{i}\delta_2)\big(D'[\mathrm{i}(2a)^{-1}] - P'[\mathrm{i}(2a)^{-1}]\big)}{4a(1 + 2\mathrm{i}a\xi)} + \frac{(\delta_2 + \mathrm{i}\delta_3)D[\mathrm{i}(2a)^{-1}]D'[\mathrm{i}(2a)^{-1}]}{1 + 2\mathrm{i}a\xi},$$

$$\xi \in \Omega_1; \quad (20)$$

$$\frac{\kappa+1}{2\mu}\varphi_2(\xi) = -\delta_1\omega(\xi) - (\delta_2 + \mathrm{i}\delta_3)P(\xi) - (\delta_2 - \mathrm{i}\delta_3)\frac{\omega(\xi)}{\bar{\omega}'(\xi)}\big(\overline{D}'(\xi) - \overline{P}'(\xi)\big)$$

$$+ 2\delta_1\big(\overline{D}(\xi) - \overline{P}(\xi)\big) + (\delta_2 - \mathrm{i}\delta_3)\left(\frac{\overline{D}(\xi)\overline{D}'(\xi)}{\bar{\omega}'(\xi)} - \overline{Q}(\xi)\right)$$

$$- \frac{3(\delta_3 + \mathrm{i}\delta_2)\big(\overline{D'[\mathrm{i}(2a)^{-1}]} - \overline{P'[\mathrm{i}(2a)^{-1}]}\big)}{4a(1 - 2\mathrm{i}a\xi)} - \frac{(\delta_2 - \mathrm{i}\delta_3)\overline{D[\mathrm{i}(2a)^{-1}]D'[\mathrm{i}(2a)^{-1}]}}{1 - 2\mathrm{i}a\xi},$$

$$\frac{\kappa+1}{2\mu}\psi_2(\xi) = -\frac{\kappa+1}{2\mu}\frac{\bar{\omega}(\xi)\varphi_2'(\xi)}{\omega'(\xi)} + (\delta_2 - \mathrm{i}\delta_3)\omega(\xi) + 2\delta_1 P(\xi) + (\delta_2 + \mathrm{i}\delta_3)Q(\xi)$$

$$- \delta_1\bar{\omega}(\xi) - (\delta_2 + \mathrm{i}\delta_3)\frac{\bar{\omega}(\xi)P'(\xi)}{\omega'(\xi)} - (\delta_2 - \mathrm{i}\delta_3)\big(\overline{D}(\xi) - \overline{P}(\xi)\big)$$

$$+ \frac{3(\delta_3 - \mathrm{i}\delta_2)\big(D'[\mathrm{i}(2a)^{-1}] - P'[\mathrm{i}(2a)^{-1}]\big)}{4a(1 + 2\mathrm{i}a\xi)} + \frac{(\delta_2 + \mathrm{i}\delta_3)D[\mathrm{i}(2a)^{-1}]D'[\mathrm{i}(2a)^{-1}]}{1 + 2\mathrm{i}a\xi},$$

$$\xi \in \Omega_2; \quad (21)$$

For a thermal inclusion ($\varepsilon_{11}^* = \varepsilon_{22}^*$, $\varepsilon_{12}^* = 0$ or $\delta_2 = \delta_3 = 0$; see [Ru 1999]), Equations (20) and (21) simplify to

$$\frac{\kappa + 1}{2\mu} \varphi_1(\xi) = 2\delta_1\big(\bar{D}(\xi) - \bar{P}(\xi)\big),$$

$$\frac{\kappa + 1}{2\mu} \psi_1(\xi) = -2\delta_1\big(D(\xi) - P(\xi)\big) - 2\delta_1 \frac{\bar{\omega}(\xi)}{\omega'(\xi)}\big(\bar{D}'(\xi) - \bar{P}'(\xi)\big), \quad \xi \in \Omega_1; \tag{22}$$

$$\frac{\kappa + 1}{2\mu} \varphi_2(\xi) = -\delta_1\omega(\xi) + 2\delta_1\big(\bar{D}(\xi) - \bar{P}(\xi)\big),$$

$$\frac{\kappa + 1}{2\mu} \psi_2(\xi) = 2\delta_1 P(\xi) - 2\delta_1 \frac{\bar{\omega}(\xi)}{\omega'(\xi)}\big(\bar{D}'(\xi) - \bar{P}'(\xi)\big), \quad \xi \in \Omega_1. \tag{23}$$

When $a = 0$ (straight boundary), the results in (20)–(23) recover those by [Ru 1999] for a half-plane.

3.2. Anti-plane eigenstrains (ε_{31}^*, ε_{32}^*).
In this case, the boundary value problem in the ξ-plane takes the following form:

$$\begin{aligned} f_1(\xi) + \overline{f_1(\xi)} &= f_2(\xi) + \overline{f_2(\xi)}, \\ f_1(\xi) - \overline{f_1(\xi)} &= f_2(\xi) - \overline{f_2(\xi)} + 2(\varepsilon_{32}^* + i\varepsilon_{31}^*)\omega(\xi) - 2(\varepsilon_{32}^* - i\varepsilon_{31}^*)\overline{\omega(\xi)}, \quad \xi \in L; \end{aligned} \tag{24a}$$

$$f_1(\xi) + \overline{f_1(\xi)} = 0, \quad \operatorname{Im}\xi = 0^-; \tag{24b}$$

$$f_1(\xi) \cong O(1), \quad |\xi| \to \infty. \tag{24c}$$

The two interface conditions in (24a) can be rewritten as

$$f_1(\xi) + (\varepsilon_{32}^* - i\varepsilon_{31}^*)\big(D(\xi) - P(\xi)\big) = f_2(\xi) + (\varepsilon_{32}^* + i\varepsilon_{31}^*)\omega(\xi) - (\varepsilon_{32}^* - i\varepsilon_{31}^*)P(\xi), \quad \xi \in L, \tag{25}$$

where $D(\xi)$ and $P(\xi)$ have been defined in (12) and (13).

We now introduce the auxiliary function $h(\xi)$ defined by

$$h(\xi) = \begin{cases} f_1(\xi) + (\varepsilon_{32}^* - i\varepsilon_{31}^*)\big(D(\xi) - P(\xi)\big), & \xi \in \Omega_1; \\ f_2(\xi) + (\varepsilon_{32}^* + i\varepsilon_{31}^*)\omega(\xi) - (\varepsilon_{32}^* - i\varepsilon_{31}^*)P(\xi), & \xi \in \Omega_2. \end{cases} \tag{26}$$

It is seen from the above definition and (25) that $h(\xi)$ is continuous across L and then analytic in the lower half ξ-plane including the point at infinity. The traction-free condition in (24b) can be expressed in terms of $h(\xi)$ as follows:

$$h^-(\xi) - (\varepsilon_{32}^* + i\varepsilon_{31}^*)\big(\bar{D}(\xi) - \bar{P}(\xi)\big) = -\bar{h}^+(\xi) + (\varepsilon_{32}^* - i\varepsilon_{31}^*)\big(D(\xi) - P(\xi)\big), \quad \operatorname{Im}\xi = 0. \tag{27}$$

The left and right sides of (27) are again analytic in the lower and upper half-planes, respectively, including the point at infinity. As above, by applying Liouville's theorem, the left and right sides of (27) should be identically zero. Thus, we arrive at the following expression for $h(\xi)$:

$$h(\xi) = (\varepsilon_{32}^* + i\varepsilon_{31}^*)[\bar{D}(\xi) - \bar{P}(\xi)], \quad \operatorname{Im}\xi \le 0. \tag{28}$$

It then follows from (26) and (28) that

$$
\begin{aligned}
f_1(\xi) &= (\varepsilon_{32}^* + \mathrm{i}\varepsilon_{31}^*)[\overline{D}(\xi) - \overline{P}(\xi)] - (\varepsilon_{32}^* - \mathrm{i}\varepsilon_{31}^*)[D(\xi) - P(\xi)], \quad \xi \in \Omega_1; \\
f_2(\xi) &= (\varepsilon_{32}^* + \mathrm{i}\varepsilon_{31}^*)[\overline{D}(\xi) - \overline{P}(\xi)] - (\varepsilon_{32}^* + \mathrm{i}\varepsilon_{31}^*)\omega(\xi) + (\varepsilon_{32}^* - \mathrm{i}\varepsilon_{31}^*)P(\xi), \quad \xi \in \Omega_2;
\end{aligned}
\tag{29}
$$

It is clear that when the subdomain undergoes only anti-plane eigenstrains, the expressions for the two analytic functions $f_1(\xi)$ and $f_2(\xi)$ are relatively simple.

4. Examples

In this section, several examples will be presented to demonstrate the general solutions obtained in the previous section.

4.1. $\xi \in L$ is a circle. When $\xi \in L$ is a circle described by

$$
|\xi - \xi_0| = R, \quad \xi \in L,
\tag{30}
$$

the explicit expressions for $D(\xi)$, $D(\xi)D'(\xi)/\omega'(\xi)$, $P(\xi)$ and $Q(\xi)$ are given by

$$
\begin{aligned}
D(\xi) &= \frac{R^2(1 - 2\mathrm{i}a\bar{\xi}_0)}{\xi - \xi_0} - \frac{\mathrm{i}aR^4}{(\xi - \xi_0)^2} + \bar{\xi}_0 - \mathrm{i}a\bar{\xi}_0^2, \\
\frac{D(\xi)D'(\xi)}{\omega'(\xi)} &= \frac{1}{1 + 2\mathrm{i}a\xi}\left[-\frac{R^2(\bar{\xi}_0 - \mathrm{i}a\bar{\xi}_0^2)(1 - 2\mathrm{i}a\bar{\xi}_0)}{(\xi - \xi_0)^2} + \frac{R^2(-1 + 6\mathrm{i}a\bar{\xi}_0 + 6a^2\bar{\xi}_0^2)}{(\xi - \xi_0)^3} \right. \\
&\qquad\qquad\qquad \left. + \frac{3\mathrm{i}aR^6(1 - 2\mathrm{i}a\bar{\xi}_0)}{(\xi - \xi_0)^4} + \frac{2a^2R^8}{(\xi - \xi_0)^5} \right],
\end{aligned}
\tag{31}
$$

$$
P(\xi) = \bar{\xi}_0 - \mathrm{i}a\bar{\xi}_0^2, \quad Q(\xi) = 0.
$$

By substituting the above expressions into (20), (21) and (29), we arrive at the six analytic functions $\varphi_j(\xi)$, $\psi_j(\xi)$, $f_j(\xi)$, $j = 1, 2$. We emphasize that although $\xi \in L$ is a circle, $z \in \Gamma$ is of irregular shape. For a thermal inclusion, the hoop stress along the parabola and the average mean stress within the inclusion are given explicitly by

$$
\sigma_{tt} = -\frac{16\mu\delta_1}{\kappa + 1}\,\mathrm{Re}\left\{ \frac{1}{1 + 2\mathrm{i}ax_1}\left[\frac{R^2(1 + 2\mathrm{i}a\xi_0)}{(x_1 - \bar{\xi}_0)^2} + \frac{2\mathrm{i}aR^4}{(x_1 - \bar{\xi}_0)^3} \right] \right\} \quad \text{on } x_2 = ax_1^2,
\tag{32}
$$

$$
\langle \sigma_{11} + \sigma_{22} \rangle = \frac{4\mu\delta_1}{\kappa + 1}\left[\frac{R^2}{(\mathrm{Im}\,\xi_0)^2} + \frac{aR^4}{(\mathrm{Im}\,\xi_0)^3}\frac{1 - 2a\,\mathrm{Im}\,\xi_0}{|1 + 2\mathrm{i}a\xi_0|^2} - 2 \right],
\tag{33}
$$

where $\langle \cdot \rangle$ denotes the average. Although the thermal inclusion is of irregular shape, an analytical expression for the average mean stress inside the inclusion can be derived in view of the fact that $\xi \in \Omega_2$ is circular. In the following numerical studies of (32) and (33) (Figures 3–6), it is assumed that $\delta_1 > 0$.

Figures 3 and 4 illustrate the hoop stress distributions along the parabola for different values of $a\xi_0$ with $aR = 1$. In Figure 3, the center of the circle $\xi \in L$ lies on the negative imaginary axis (i.e., $\mathrm{Re}\,\xi_0 = 0$); whilst in Figure 4, the circle $\xi \in L$ is just touching the real axis (i.e., $\mathrm{Im}\,\xi_0 = -R$). It is observed from Figure 3 that: (i) the hoop stress is an even function of x_1, which is intuitively consistent; (ii) the magnitude of the hoop stress reduces as the center of the circle $\xi \in L$ moves further away from the real axis in the ξ-plane; (iii) the hoop stress is tensile ($\sigma_{tt} > 0$) when $a|x_1|$ is sufficiently small, but
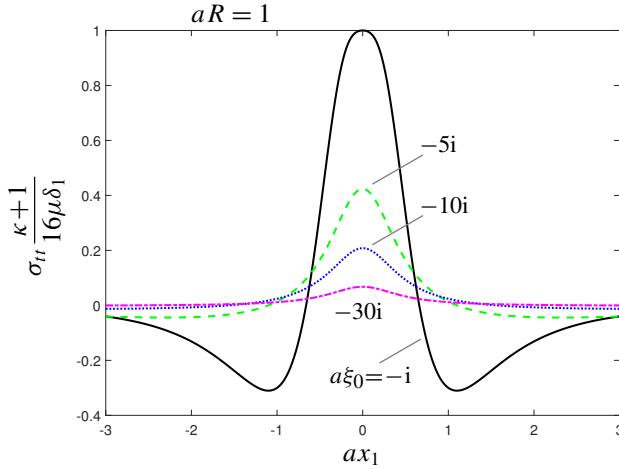
Figure 3. The hoop stress distributions along the parabola for $a\xi_0$ taking the values $-i$, $-5i$, $-10i$, $-30i$, with $aR = 1$ and $\operatorname{Re}\xi_0 = 0$.
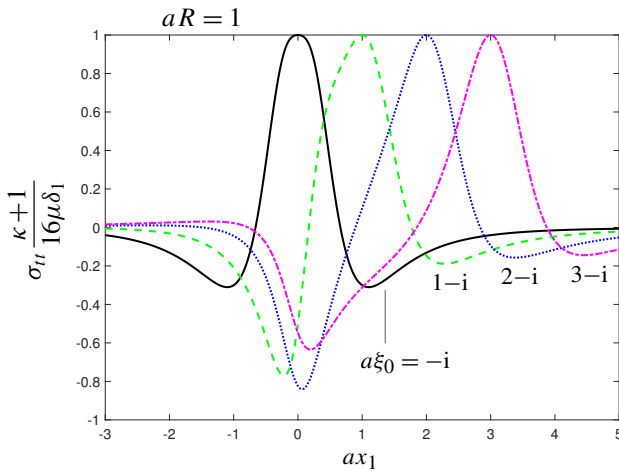

Figure 4. The hoop stress distributions along the parabola for $a\xi_0$ taking the values $-i$, $1 - i$, $2 - i$, and $3 - i$, with $aR = 1$ and $\operatorname{Im}\xi_0 = -R$.

compressive ($\sigma_{tt} < 0$) when $a|x_1|$ becomes sufficiently large; (iv) the maximum value of the hoop stress:

$$\max\{\sigma_{tt}\} = \frac{16\mu\delta_1}{\kappa + 1} \frac{(aR)^2[|a\xi_0| + 2|a\xi_0|^2 - 2(aR)^2]}{|a\xi_0|^3} > 0, \tag{34}$$

occurs at $x_1 = 0$ for a fixed value of $a\xi_0$. It is observed from Figure 4 that: (i) when the center of the circle is not on the imaginary axis, the hoop stress is no longer an even function of x_1; (ii) the maximum value of the hoop stress $\max = \{\sigma_{tt}\} = 16\mu\delta_1/(\kappa + 1)$ occurs at $x_1 = \operatorname{Re}\xi_0$ for a fixed value of $a\xi_0$; (iii) the magnitude of the compressive hoop stress is considerable when $a\operatorname{Re}\xi_0 = 1 \sim 2$.

Figure 5 plots the average mean stress within the inclusion as a function of $a\operatorname{Im}\xi_0$ and aR with $\operatorname{Re}\xi_0 = 0$ (the center of the circle $\xi \in L$ lies on the negative imaginary axis). It is seen from Figure 5 that:
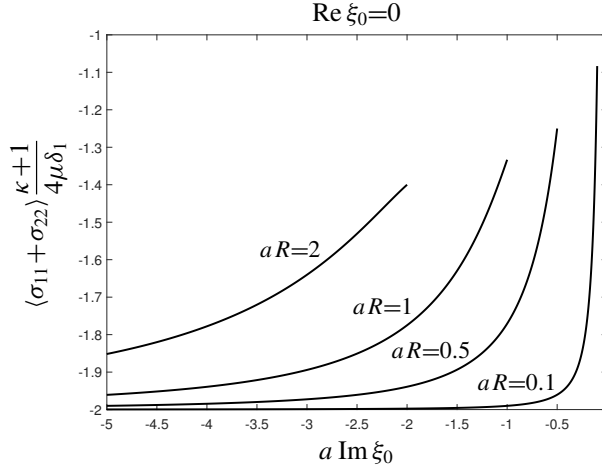
Figure 5. The average mean stress within the inclusion as a function of $a \operatorname{Im} \xi_0$ and aR with $\operatorname{Re} \xi_0 = 0$.
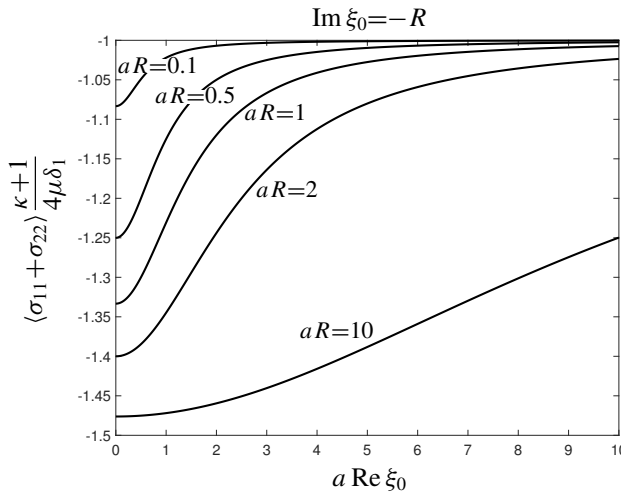
Figure 6. The average mean stress within the inclusion as a function of $a \operatorname{Re} \xi_0$ and aR with $\operatorname{Im} \xi_0 = -R$.

(i) $\langle \sigma_{11} + \sigma_{22} \rangle$ is an increasing function of both $a \operatorname{Im} \xi_0$ and aR; (ii) $\langle \sigma_{11} + \sigma_{22} \rangle$ is always negative and reaches its maximum when $\xi_0 = -iR$; (iii) as $a \operatorname{Im} \xi_0 \to -\infty$ or $aR \to 0$, $\langle \sigma_{11} + \sigma_{22} \rangle \cong -8\mu\delta_1/(\kappa+1)$, which is simply the value of a circular thermal inclusion in a homogeneous plane [Ru 1999]. Figure 6 plots the average mean stress within the inclusion as a function of $a \operatorname{Re} \xi_0$ and aR with $\operatorname{Im} \xi_0 = -R$ (the inclusion just touches the parabola). It is seen from Figure 6 that: (i) $\langle \sigma_{11} + \sigma_{22} \rangle$ is an increasing function of $a \operatorname{Re} \xi_0$ and a decreasing function of aR; (ii) $\langle \sigma_{11} + \sigma_{22} \rangle$ is always negative, and

$$\min\{\langle \sigma_{11} + \sigma_{22} \rangle\} = -\frac{4\mu\delta_1}{\kappa+1} \frac{1+3aR}{1+2aR} \geq -\frac{6\mu\delta_1}{\kappa+1}, \tag{35}$$

occurs at $\operatorname{Re} \xi_0 = 0$; (iii) $\langle \sigma_{11} + \sigma_{22} \rangle \cong -4\mu\delta_1/(\kappa+1)$ as $a \operatorname{Re} \xi_0 \to \infty$ or $aR \to 0$.

4.2. *A thermal inclusion with $\xi \in L$ describing an ellipse.* We consider a thermal inclusion. In addition, $\xi \in L$ is an ellipse described by

$$\xi = w(\eta) = R\left(\eta + \frac{m}{\eta}\right) + \xi_0, \quad R > 0, \quad 0 < |m| < 1, \quad |\eta| = 1, \tag{36}$$

in which m and ξ_0 are complex numbers.

In this case, $D(\xi)$, $P(\xi)$ and $D(\xi) - P(\xi)$ are determined to be

$$D(\xi) = (\bar{m} - m^{-1})[1 - 2ia\bar{\xi}_0 - ia(\bar{m} + m^{-1})(\xi - \xi_0)]\left[\frac{\xi - \xi_0}{2} + \left(\frac{(\xi - \xi_0)^2}{4} - mR^2\right)^{1/2}\right]$$

$$+ \bar{\xi}_0 + ia\left[R^2 m^{-1}(1 - |m|^2)^2 - \bar{\xi}_0^2\right] + m^{-1}(\xi - \xi_0)\left[1 - 2ia\bar{\xi}_0 - iam^{-1}(\xi - \xi_0)\right],$$

$$P(\xi) = -ia\bar{m}^2\xi^2 + \bar{m}[1 - 2ia(\bar{\xi}_0 - \bar{m}\xi_0)]\xi + \bar{\xi}_0 - \bar{m}\xi_0 + ia\left[2R^2\bar{m}(|m|^2 - 1) - (\bar{\xi}_0 - \bar{m}\xi_0)^2\right],$$

$$D(\xi) - P(\xi) = (\bar{m} - m^{-1})[1 - 2ia\bar{\xi}_0 - ia(\bar{m} + m^{-1})(\xi - \xi_0)]\left[\left(\frac{(\xi - \xi_0)^2}{4} - mR^2\right)^{1/2} - \frac{\xi - \xi_0}{2}\right]$$

$$- iamR^2(\bar{m}^2 - m^{-2}). \tag{37}$$

By substituting the above into (22) and (23), we arrive at the two pairs of analytic functions $\varphi_j(\xi)$, $\psi_j(\xi)$, $j = 1, 2$. We emphasize that although $\xi \in L$ is an ellipse (see Figure 2), $z \in \Gamma$ is non-elliptical (see Figure 1). The explicit expressions for the hoop stress along the parabola and the mean stress within the thermal inclusion are finally found to be

$$\sigma_{tt} = \frac{8\mu\delta_1}{\kappa + 1} \text{Re}\left\{\frac{(m - \bar{m}^{-1})(1 + 2ia\xi_0)}{1 + 2iax_1}\left[\frac{x_1 - \bar{\xi}_0}{\sqrt{(x_1 - \bar{\xi}_0)^2 - 4\bar{m}R^2}} - 1\right]\right\}$$

$$- \frac{32\mu\delta_1 aR^2}{\kappa + 1} \text{Im}\left\{\frac{\bar{m}(m^2 - \bar{m}^{-2})}{1 + 2iax_1}\left[\frac{1}{\sqrt{(x_1 - \bar{\xi}_0)^2 - 4\bar{m}R^2}} - \frac{2}{x_1 - \bar{\xi}_0 + \sqrt{(x_1 - \bar{\xi}_0)^2 - 4\bar{m}R^2}}\right]\right\},$$

$$\text{on } x_2 = ax_1^2, \tag{38}$$

$$\sigma_{11} + \sigma_{22} = -\frac{8\mu\delta_1}{\kappa + 1} + \frac{8\mu\delta_1}{\kappa + 1} \text{Re}\left\{\frac{(m - \bar{m}^{-1})(1 + 2ia\xi_0)}{1 + 2ia\xi}\left[\frac{\xi - \bar{\xi}_0}{\sqrt{(\xi - \bar{\xi}_0)^2 - 4\bar{m}R^2}} - 1\right]\right\}$$

$$- \frac{32\mu\delta_1 aR^2}{\kappa + 1} \text{Im}\left\{\frac{\bar{m}(m^2 - \bar{m}^{-2})}{1 + 2ia\xi}\left[\frac{1}{\sqrt{(\xi - \bar{\xi}_0)^2 - 4\bar{m}R^2}} - \frac{2}{\xi - \bar{\xi}_0 + \sqrt{(\xi - \bar{\xi}_0)^2 - 4\bar{m}R^2}}\right]\right\},$$

$$\xi \in \Omega_2. \tag{39}$$

5. Conclusions

A novel procedure is presented to derive analytic solutions for the Eshelby's problem of an inclusion of arbitrary shape in an isotropic plane with parabolic boundary. First, a conformal mapping function, which maps the region with the parabolic boundary in the physical plane onto the lower half of the image ξ-plane, is introduced in (8). In the ξ-plane, an auxiliary function $D(\xi)$ is then constructed via (12). The technique of analytic continuation is further applied with this auxiliary function to derive the analytic functions $\varphi_j(\xi)$, $\psi_j(\xi)$, $f_j(\xi)$, $j = 1, 2$. In contrast to the method used by [Ru 1999] in the analysis of

the corresponding "straight boundary problems", our analysis remains in the ξ-plane where the parabola is conveniently mapped onto the real axis.

Acknowledgements

References

[England 1971] A. H. England, *Complex variable methods in elasticity*, Wiley, London, 1971.

[Muskhelishvili 1953] N. I. Muskhelishvili, *Some basic problems of the mathematical theory of elasticity*, Noordhoff, Groningen, 1953.

[Ru 1999] C. Q. Ru, "Analytic solution for Eshelby's problem of an inclusion of arbitrary shape in a plane or half-plane", *J. Appl. Mech.* (*ASME*) **66** (1999), 315–322.

[Ru 2000] C. Q. Ru, "Eshelby's problem for two-dimensional piezoelectric inclusions of arbitrary shape", *Proc. Roy. Soc. London A* **456** (2000), 1051–1068.

[Ru 2003] C. Q. Ru, "Eshelby inclusion of arbitrary shape in an anisotropic plane/half-plane", *Acta Mech.* **160** (2003), 219–234.

[Savin 1961] G. N. Savin, *Stress concentration around holes*, Pergamon Press, London, 1961.

[Ting 1996] T. C. T. Ting, *Anisotropic elasticity: theory and applications*, Oxford University Press, New York, 1996.

[Ting et al. 2001] T. C. T. Ting, Y. Hu, and H. O. K. Kirchner, "Anisotropic elastic materials with a parabolic or hyperbolic boundary: a classical problem revisited", *J. Appl. Mech.* (*ASME*) **68** (2001), 537–542.

[Wang 2004] X. Wang, "Eshelby's problem of an inclusion of arbitrary shape in a decagonal quasicrystalline plane or half-plane", *Int. J. Eng. Sci.* **42** (2004), 1911–1930.

[Wang and Schiavone 2015] X. Wang and P. Schiavone, "Eshelby's problem for infinite, semi-infinite and two bonded semi-infinite laminated anisotropic thin plates", *Arch. Appl. Mech.* **85** (2015), 573–585.

[Wang and Zhou 2014] X. Wang and K. Zhou, "An inclusion of arbitrary shape in an infinite or semi-infinite isotropic multi-layered plate", *Int. J. Appl. Mech.* **6** (2014), art. id 1450001 (21 pages).

[Zhou et al. 2013] K. Zhou, H. J. Hoh, X. Wang, L. M. Keer, J. H. L. Pang, B. Song, and Q. J. Wang, "A review of recent works on inclusions", *Mech. Mater.* **60** (2013), 144–158.

XU WANG: xuwang@ecust.edu.cn
School of Mechanical and Power Engineering, East China University of Science and Technology, 130 Meilong Road, Shanghai, 200237, China

LIANG CHEN: liangchen5962@mail.ecust.edu.cn
School of Mechanical and Power Engineering, East China University of Science and Technology, 130 Meilong Road, Shanghai, 200237, China

PETER SCHIAVONE: p.schiavone@ualberta.ca
Department of Mechanical Engineering, University of Alberta, 10-203 Donadeo Innovation Center for Engineering, 9211-116 Street NW, Edmonton AB T6G 1H9, Canada

JOURNAL OF MECHANICS OF MATERIALS AND STRUCTURES

Founded by Charles R. Steele and Marie-Louise Steele

Cover photo: Mando Gomez, www.mandolux.com

See msp.org/jomms for submission guidelines.

Journal of Mechanics of Materials and Structures